Design of Mach-Zehnder Interferometers for Silicon Photonics at 1550 nm Wavelength

Sayed Omid Sayedaghaee (2025/04)

username : somids

Introduction

Silicon photonics provides a promising platform for integrated optical circuits due to its high integration density, compatibility with existing CMOS fabrication processes, and low cost. In this project, the design of Mach-Zehnder Interferometers (MZIs) tailored for transverse electric (TE) and transverse magnetic (TM) polarization modes at the commonly used telecommunications wavelengths of 1550 nm is presented. The designs utilize grating couplers for light input, Y-branch splitters to divide the light in the MZI arms, and directional couplers for combining the light at the output. The aim is to design efficient, low-loss devices while ensuring high-performance operation across both wavelengths and polarization modes. The designs were fabricated and the analyses for simulation versus measurement are performed for one of the TE designs.

Theory

A Mach-Zehnder Interferometer (MZI) is a key element in integrated optics, including two waveguides that split, recombine, and interfere. The operation of MZIs is based on the interference between two split beams of light, with phase shifts in the arms of the interferometer leading to constructive or destructive interference at the output. The design involves three main components:

- Grating Coupler: Used to couple light from optical fibers into the silicon waveguide.
- Y-Branch Splitter: A passive device that splits light equally into two arms of the MZI.
- Directional Coupler: A coupling structure that recombines light from the two arms of the MZI.

The transfer function of MZI can be modeled using

$$F = 10\log_{10}\left(\frac{1}{4}\left|1 + e^{-i\frac{2\pi n_{eff}}{\lambda}\Delta L - \frac{\alpha}{2}\Delta L}\right|^2\right) + b$$

Where λ is wavelength, ΔL is the path length difference between the MZI arms, α is the waveguide loss, b is excess insertion loss, and n_{eff} is the effective index given by a second order Taylor expansion polynomial around the wavelength λ_0 in the middle of the spectrum:

$$n_{eff} = n_1 + n_2(\lambda - \lambda_0) + n_3(\lambda - \lambda_0)^2.$$

Here, n_1, n_2, an n_3 are representatives of effective index, group index, and dispersion, respectively. The objective is to find n_1, n_2, an n_3 via curve-fitting. The following equations for the group index, n_g, and group velocity dispersion, D, can be used to find the relationships:

$$n_g = n_{eff} - \lambda \frac{dn_{eff}}{d\lambda} = n_1 - n_2\lambda_0$$

$$D = -\frac{\lambda}{c}\frac{d^2n}{d\lambda^2} = -\frac{\lambda}{c}2n_3$$

Techniques such as peak-finding or autocorrelation could be used to find initial values required for curve-fitting. The spacing between two adjacent peaks of wavelength known as free spectral range (FSR) can be calculated via the following:

$$FSR = \frac{\lambda^2}{n_g \Delta L}.$$

Design Parameters

Four different MZI configurations, optimized for the TE and TM polarization modes at the wavelength of 1550 nm, were designed. The waveguide critical design parameters for each case are as follows:

- Waveguide geometry: The dimensions of the waveguide are chosen to ensure efficient mode propagation while minimizing losses. For both TE and TM modes, the waveguide geometry is 500x220 nm to accommodate the different mode confinement.
- Length of Arms: The arms of the MZI designs are provided in Table 1.

Case	Mode	Length mismatch	Label
1	TE	long arm: 196 μm, short arm: 136 μm ($\Delta L = 60\ nm$)	TE1*
2	TM	long arm: 170 μm, short arm: 110 μm ($\Delta L = 60\ nm$)	TM1
3	TE	long arm: 250 μm, short arm: 230 μm ($\Delta L = 20\ nm$)	TE2
4	TM	long arm: 635 μm, short arm: 455 μm ($\Delta L = 180\ nm$)	TM2

* used for measurement vs. simulation analyses

Table 1 – MZI designs for fabrication

- Directional Coupler Length: The length of the directional coupler is chosen to provide optimal coupling between the arms of the MZI.

The layout was designed using KLayout software. A screenshot of the designed devices is provided in Figure 1.

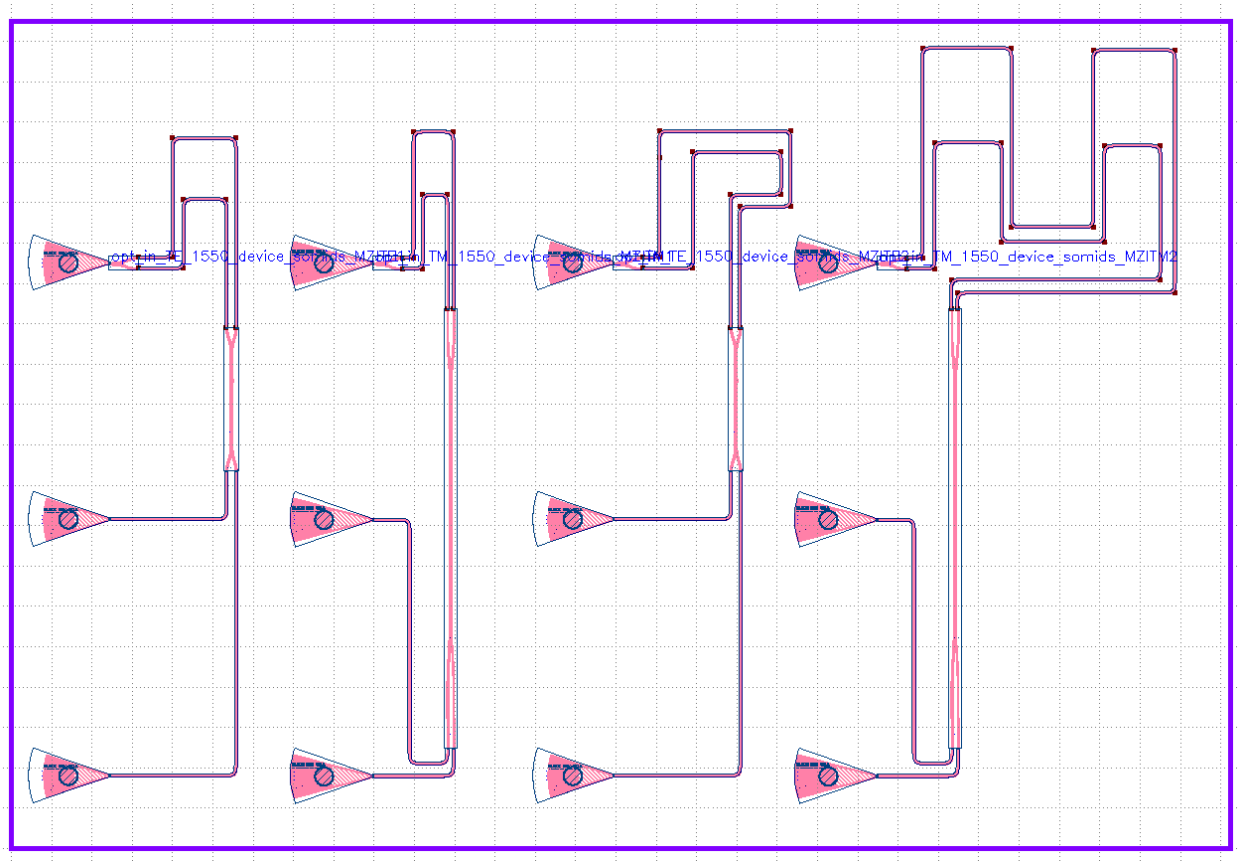

Figure 1 - KLayout design of MZI for TE and TM modes for 1550 nm

The design used for the analyses of measurement versus simulation, TE1, is the most left design demonstrated in Figure 1.

Modeling and Simulation

The designs were simulated using Lumerical Mode and Lumerical Interconnect to verify the propagation characteristics of the waveguide and the performance of the directional couplers.

First Lumerical Mode simulation was performed for the waveguide geometry of 500x220 nm (TE1) which gave the following results.

Width	Thickness	Effective Index	Group Index
500 nm	220 nm	2.4468	4.2037

Table 2 – Lumerical Mode simulation results

Then, Lumerical Interconnect simulations were performed to calculate gain, transmission, and the FSR for TE1 design. The results of such simulations are presented in the following.

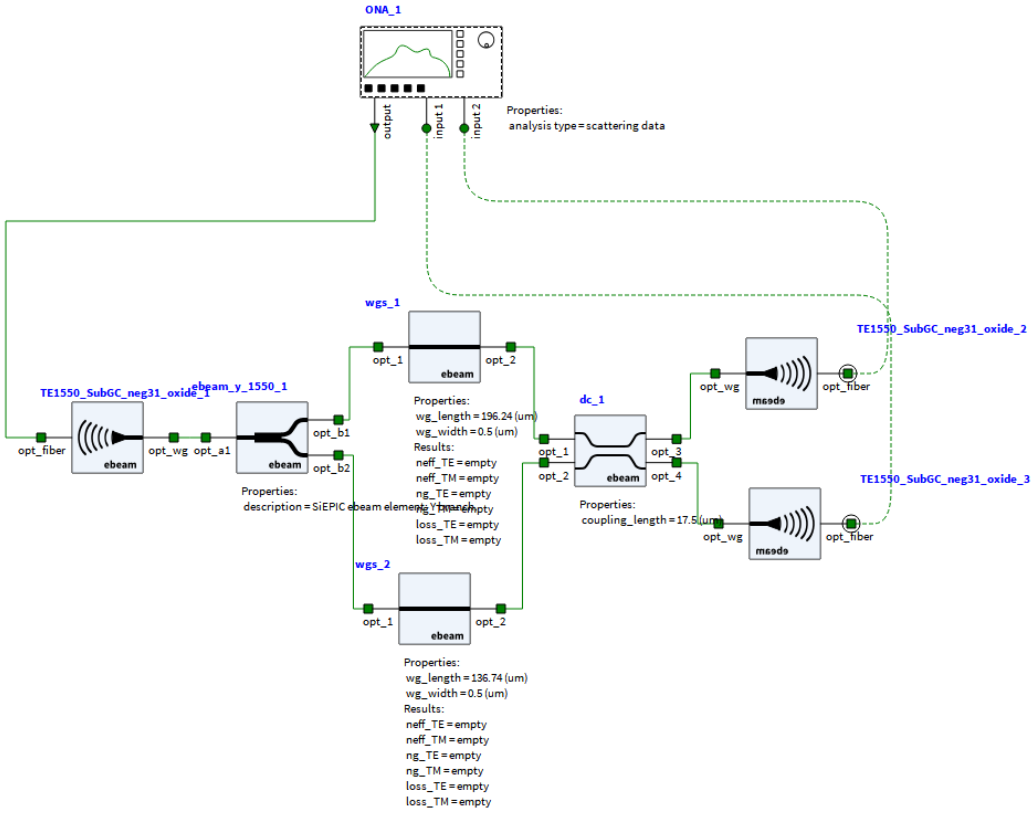

Figure 2 – Lumerical Interconnect simulation for TE1 Design

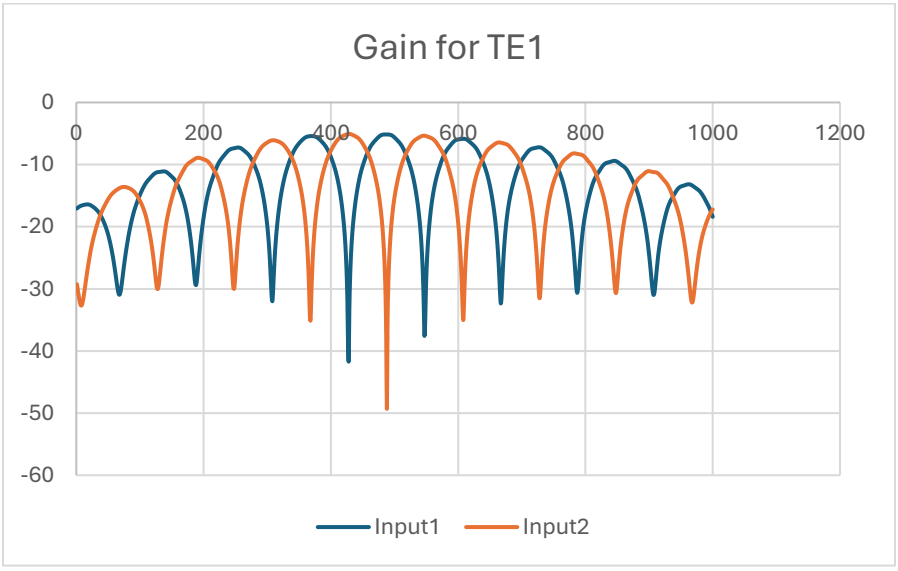

Figure 3 – Gain for TE1 Design

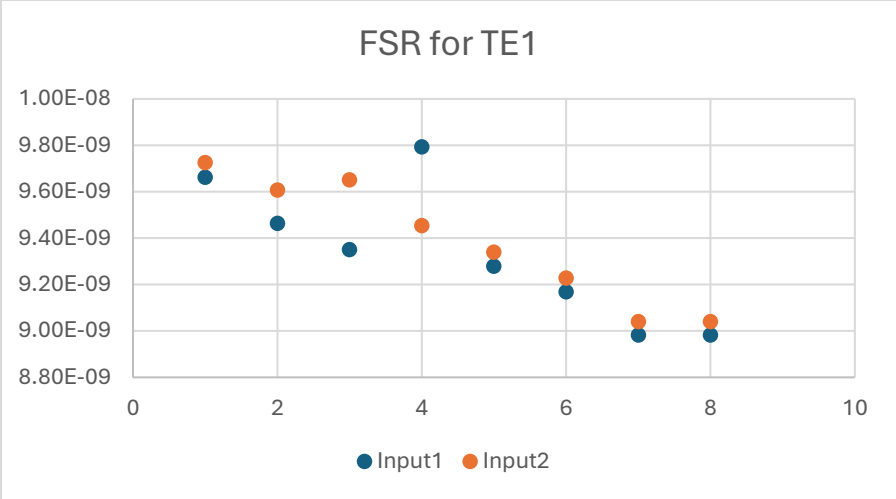

Figure 4 – FSR for TE1Design

Fabrication Process

The photonic devices were fabricated using the NanoSOI MPW fabrication process by Applied Nanotools Inc. (http://www.appliednt.com/nanosoi; Edmonton, Canada) which is based on direct-write 100 keV electron beam lithography technology. Silicon-on-insulator wafers of 200 mm diameter, 220 nm device thickness and 2 µm buffer oxide thickness are used as the base material for the fabrication. The wafer was pre-diced into square substrates with dimensions of 25x25 mm, and lines were scribed into the substrate backsides to facilitate easy separation into smaller chips once fabrication was complete. After an initial wafer clean using piranha solution (3:1 H2SO4:H2O2) for 15 minutes and water/IPA rinse, hydrogen silsesquioxane (HSQ) resist was spin-coated onto the substrate and heated to evaporate the solvent. The photonic devices were patterned using a JEOL JBX-8100FS electron beam instrument at The University of British Columbia. The exposure dosage of the design was corrected for proximity effects that result from the backscatter of electrons from exposure of nearby features. Shape writing order was optimized for efficient patterning and minimal beam drift. After the e-beam exposure and subsequent development with a tetramethylammonium sulfate (TMAH) solution, the devices were inspected optically for residues and/or defects. The chips were then mounted on a 4” handle wafer and underwent an anisotropic ICP-RIE etch process using chlorine after qualification of the etch rate. The resist was removed from the surface of the devices using a 10:1 buffer oxide wet etch, and the devices were inspected using a scanning electron microscope (SEM) to verify patterning and etch quality. A 2.2 µm oxide cladding was deposited using a plasma-enhanced chemical vapour deposition (PECVD) process based on tetraethyl orthosilicate (TEOS) at 300ºC. Reflectrometry measurements were performed

throughout the process to verify the device layer, buffer oxide and cladding thicknesses before delivery.

Measurement Description and Experimental Setup

To characterize the devices, a custom-built automated test setup [2, 6] with automated control software written in Python was used [3]. An Agilent 81600B tunable laser was used as the input source and Agilent 81635A optical power sensors as the output detectors. The wavelength was swept from 1500 to 1600 nm in 10 pm steps. A polarization maintaining (PM) fiber was used to maintain the polarization state of the light, to couple the TE polarization into the grating couplers [4]. A 90º rotation was used to inject light into the TM grating couplers [4]. A polarization maintaining fiber array was used to couple light in/out of the chip [5].

Manufacturing Variability

To consider the variations in the fabrication processes, a corner analysis is performed in which the width of the waveguide was changed from 470 nm to 510 nm while the thickness was subject change from 215.3 nm to 223.1 nm. The results for such variations is summarized in Table 3 and demonstrated Figure 5 and Figure 6.

case	width	thickness	Effective index	group index	FSR
1	470	215.3	2.372	4.2523	9.66E-09
2	470	220	2.3916	4.2634	9.46E-09
3	470	223.1	2.4061	4.2607	9.35E-09
4	500	215.3	2.4271	4.1939	9.79E-09
5	500	220	2.4468	4.2037	9.28E-09
6	500	223.1	2.4592	4.2034	9.17E-09
7	510	215.3	2.4412	4.1788	8.98E-09
8	510	220	2.4608	4.1884	8.98E-09
9	510	223.1	2.4738	4.187	9.66E-09

Table 3 – Corner analysis results for different waveguide geometries

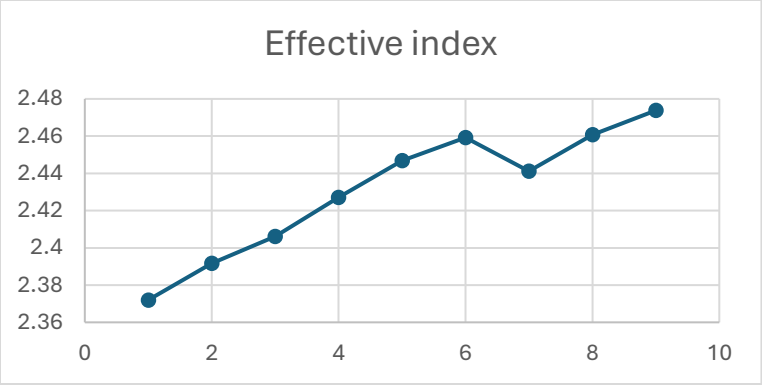

Figure 5 – Effective index results for corner analysis

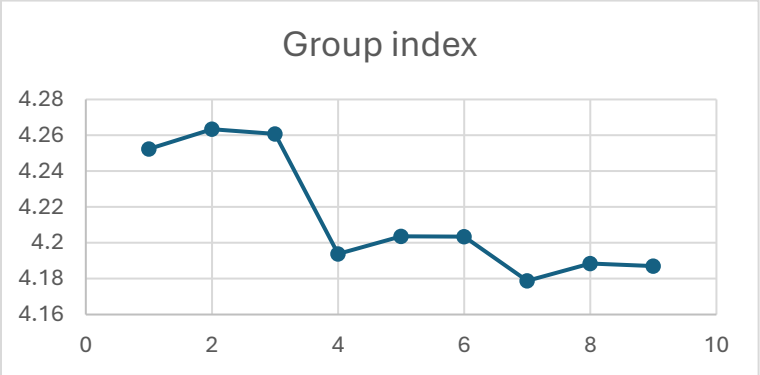

Figure 6 – Group index results for corner analysis

Experiment Results and Discussion

The MZI designs demonstrated in Figure 1 were fabricated by Applied Nanotools Inc. and the measurement results were analyzed through numerical methods based on MATLAB and Python Scripts to extract the waveguide parameters from the experimental results. Here we picked one of the designs (TE1, $\Delta L = 60\ \mu m$) to investigate overlaps between measurement and simulation. Since grating couplers have a limited bandwidth, the baseline shape should be removed using a curve-fitting method with a low-order polynomial. Here a 4^{th}-order polynomial is used for baseline corrections. The transfer function of the nominal design versus experimental measurement before and after baseline corrections are shown in Figure 7 and Figure 8, respectively.

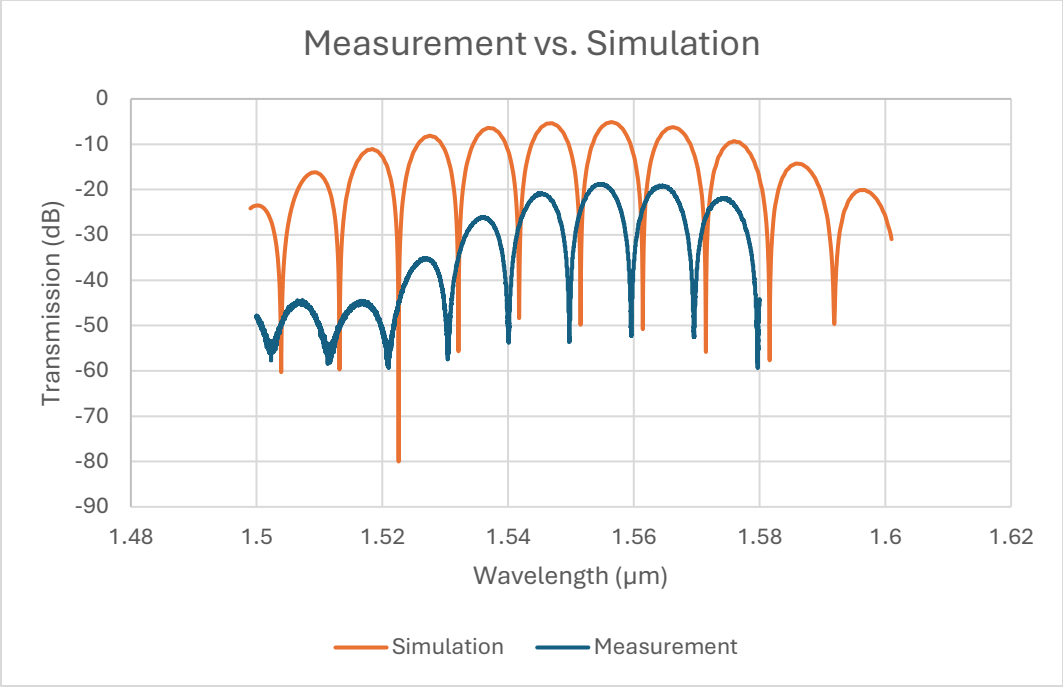

Figure 7 – Measurement vs. Simulation for TE1

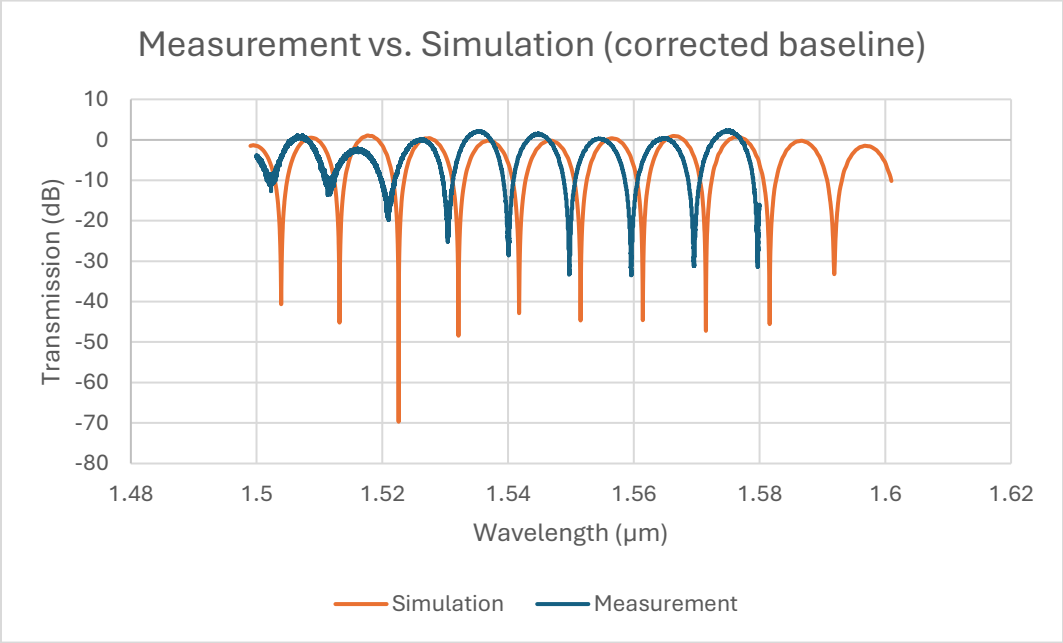

Figure 8 – Measurement vs. Simulation after baseline correction for TE1

Then, numerical fitting methods were used to extract waveguide parameters. The measurements were analyzed with two methods, peak-finding and autocorrelation, as discussed in the following.

Peak-finding method

After applying baseline corrections on the measurement results, the peaks in the spectrum were found using MATLAB find peak method. Since the minima are more precisely located the method searched and located the minima. The results are shown in Figure 9.

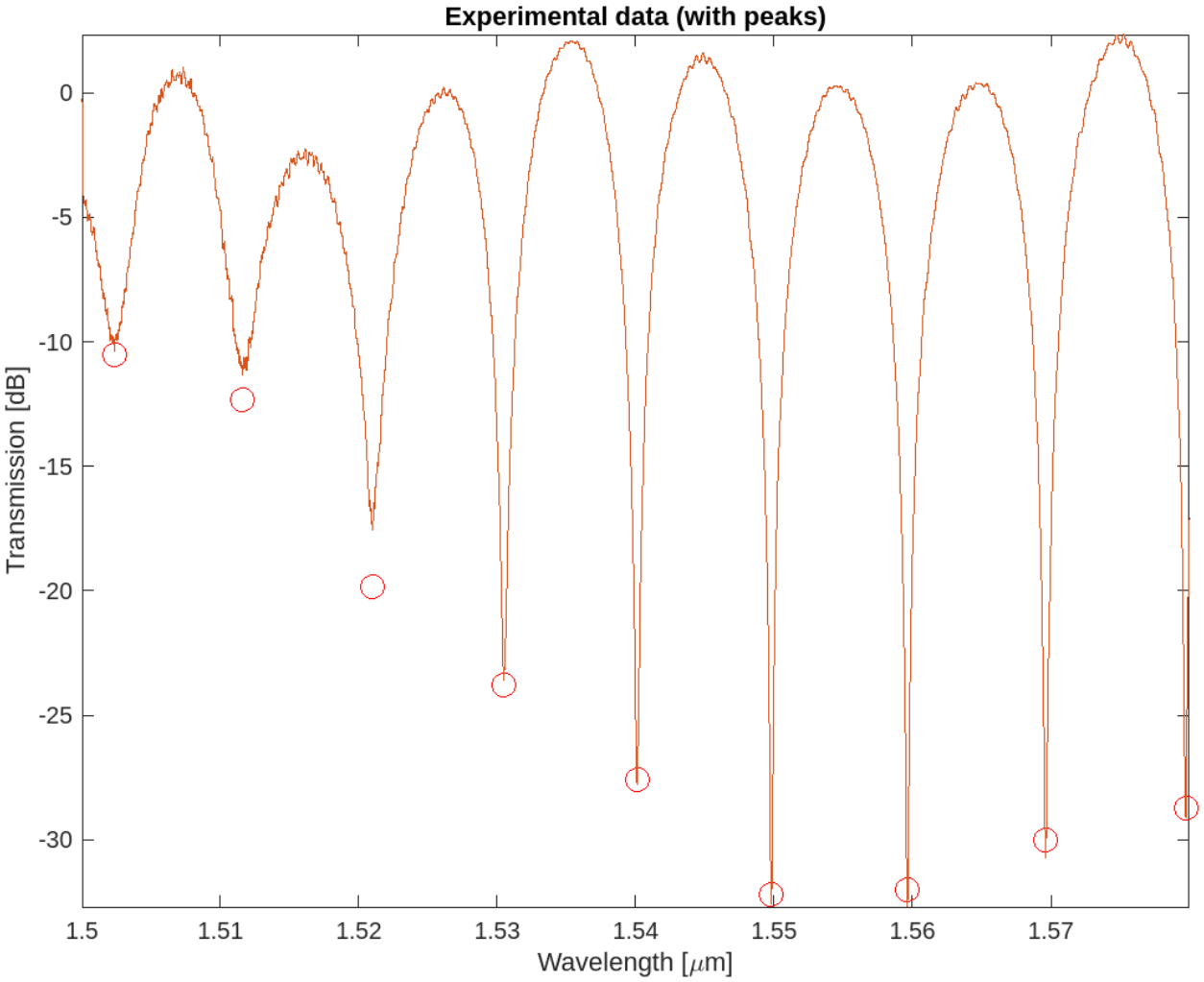

Figure 9 – Finding minima peaks in the measured spectrum (TE1)

Then free spectral range is then calculated, and based on the trend of the group index extracted at each wavelength, the initial parameters to fit the MZI model are calculated (Figure 10). As demonstrated in Figure 11, the measured data and model with initial parameters have a good correlation. Finally, group index can be plotted versus wavelength to extract the group index of the waveguide at the given wavelength (Figure 12).

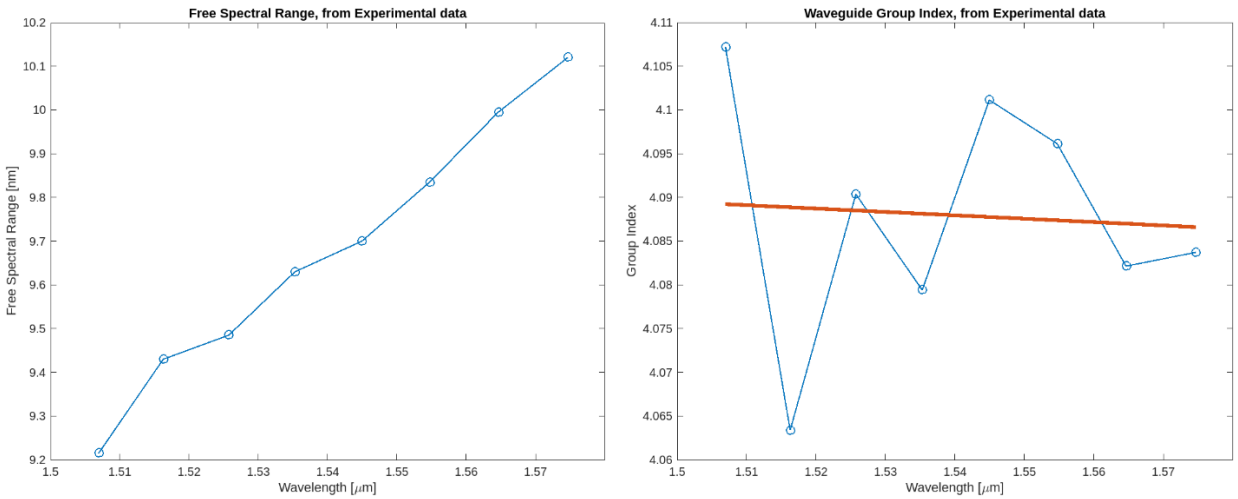

Figure 10 – Free Spectral Range vs. Wavelength (TE1), Waveguide group index trend

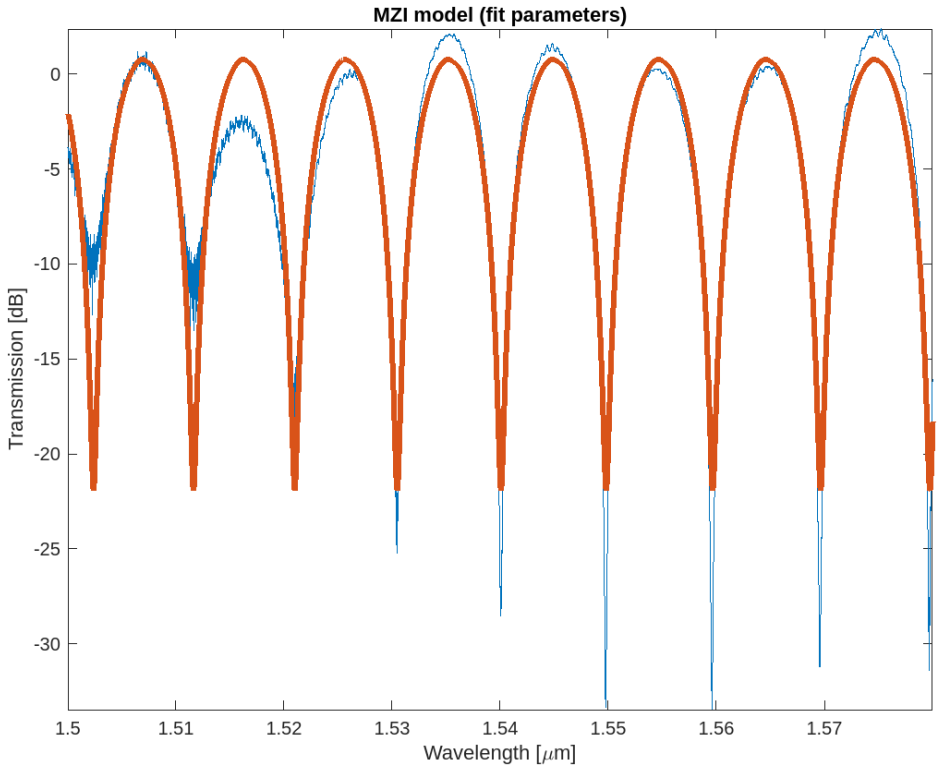

Figure 11 – Finding initial parameters for MZI fit, experiment vs. model with find peaks method

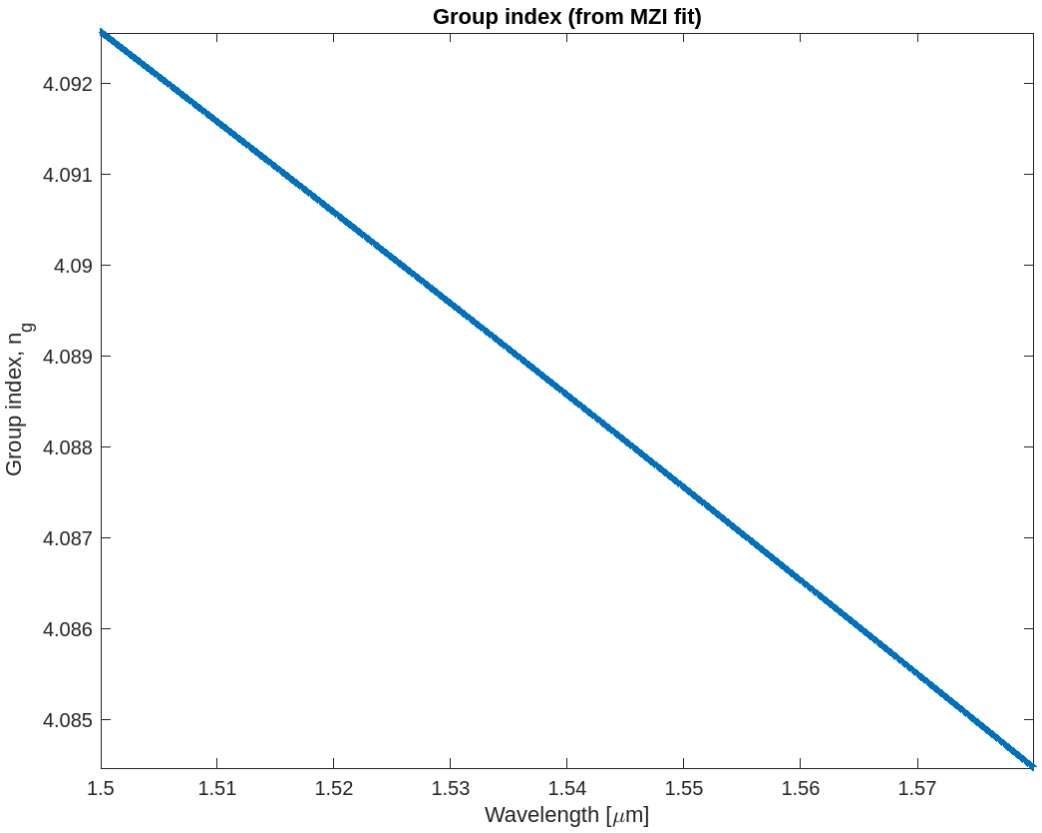

Figure 12 – Group index vs. Wavelength (TE1) – Find peaks method

The parameters extracted by MATLAB script are as follows:

- Goodness of fit, r^2 value: 0.88523
- Waveguide parameters at wavelength [um]: 1.5305
- Group index: 4.0895
- Dispersion [ps/nm/km]: -335.6275

Autocorrelation method

After applying baseline corrections on the measurement results, the autocorrelation of the spectrum is calculated as shown in Figure 13. Then initial parameters are calculated and adjusted to match the model with the measurement results (Figure 14). As shown in Figure 15, the measured data and model with initial parameters have a good correlation with the autocorrelation method as well. Finally, group index can be plotted versus wavelength to extract the group index of the waveguide at the given wavelength (Figure 16).

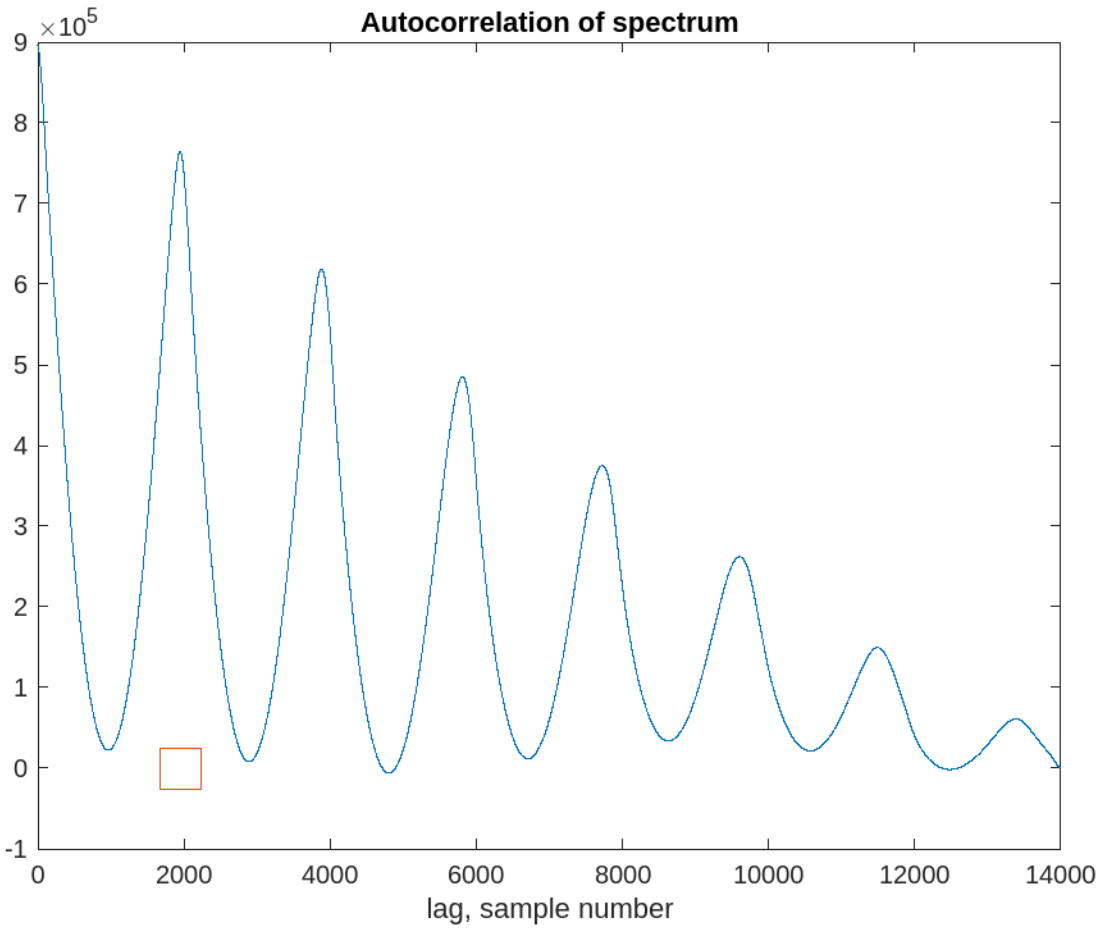

Figure 13 – Autocorrelation of the spectrum for TE1

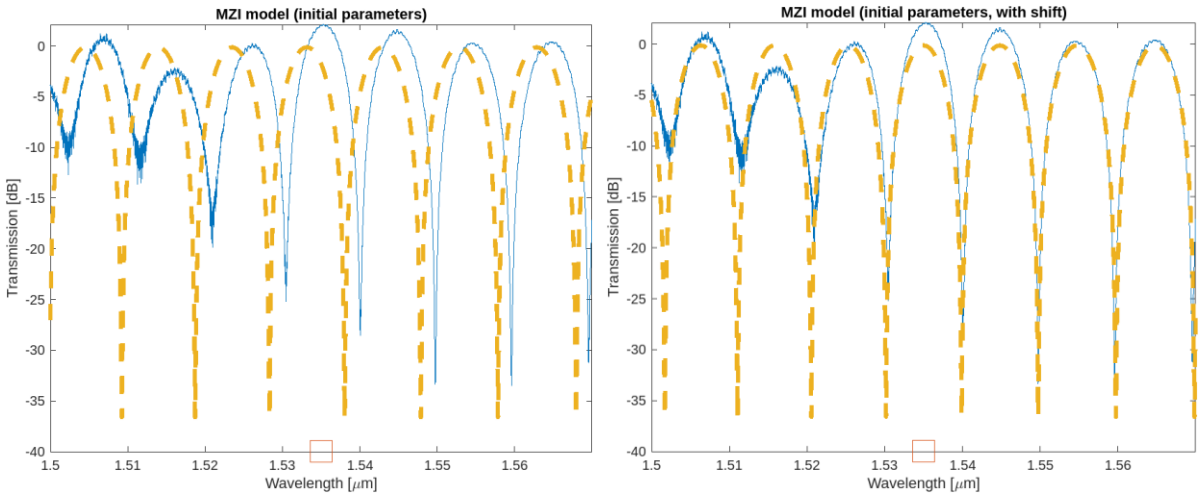

Figure 14 – Shifting the initial parameters to match the model with measurement results

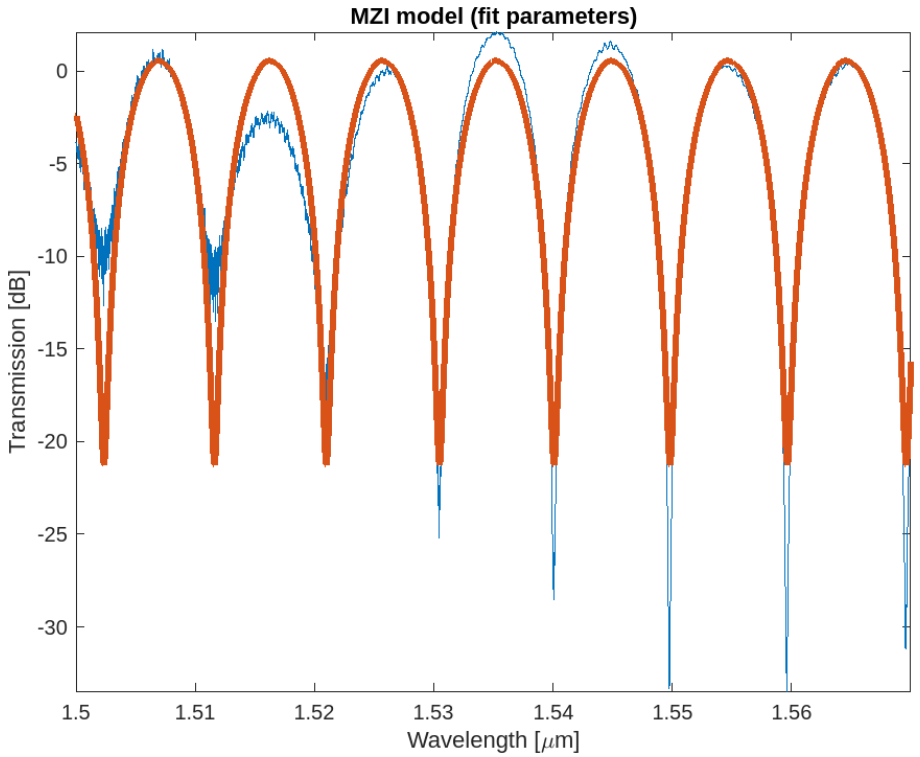

Figure 15- Finding initial parameters for MZI fit, experiment vs. model with autocorrelation method

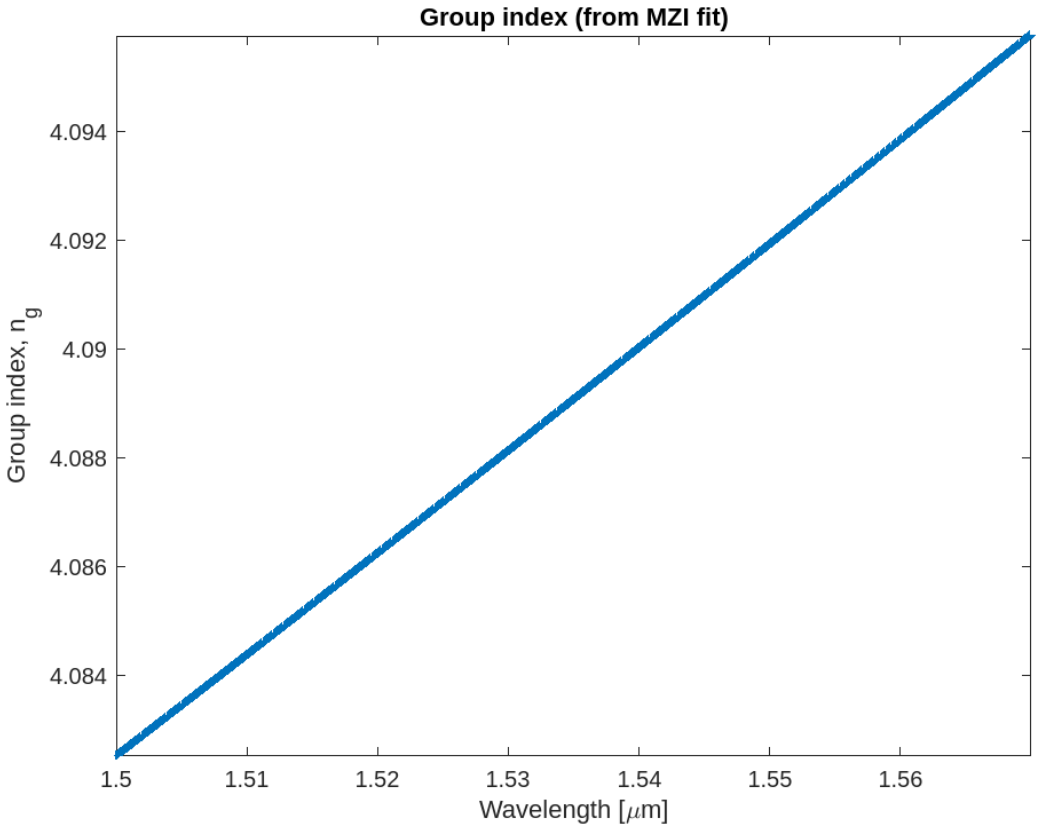

Figure 16 - Group index vs. Wavelength (TE1) – Autocorrelation method

The parameters extracted by MATLAB script are as follows:

- fsr = 9.7450e-09
- ng_av = 4.0298
- xfit = 2.4054 -1.0968 -0.0617 0.0054 1.2111
- r2 = 0.8772
- ng0 = 4.0891

analysis

The measurement analyses results and simulation outcomes are summarized in Table 4.

Case	effective index	group index	FSR
Simulation (500x220 nm)	**2.4468**	**4.2037**	**9.28E-09**
Experiment (find peaks)	2.3849	4.0895	9.68E-09
Experiment (autocorrelation)	2.4054	4.0891	9.75E-09
Experiment (average of two methods)	**2.3952**	**4.0893**	**9.72E-09**
Best matching case of corner analysis (510x215.3 nm)	**2.4412**	**4.1788**	**8.98E-09**

Table 4 – Comparison of the simulation, corner analysis, and experimental measurements

The difference between simulation of the nominal design, simulation of the best matching corner case, and measurement analyses averages are summarized in Table 5.

difference	Effective index	group index	FSR
simulation of nominal design vs. measurement	2.1%	2.7%	4.7%
simulation of best matching corner case vs. measurement	1.9%	2.1%	8.2%

Table 5 – difference between simulation and measurement

Conclusion

This project aimed to design and fabricate MZIs at 1550 nm wavelengths in silicon photonics. The inclusion of grating couplers, Y-branch splitters, and directional couplers ensured the efficient operation of the MZI. Simulation and experimental results were compared to optimize the design parameters and achieve low-loss, high-performance photonic devices suitable for telecommunication applications. The difference between the simulation and measured data found to be approximately 2% for both effective index and group index.

Acknowledgments

I acknowledge the edX UBCx Phot1x Silicon Photonics Design, Fabrication and Data Analysis course, which is supported by the Natural Sciences and Engineering Research Council of Canada (NSERC) Silicon Electronic-Photonic Integrated Circuits (SiEPIC) Program. The devices were fabricated by Applied Nanotools Inc. I also acknowledge Lumerical Solutions, Inc., Mathworks, Python, and KLayout for the design software.

References

[1] R. J. Bojko, J. Li, L. He, T. Baehr-Jones, M. Hochberg, and Y. Aida, "Electron beam lithography writing strategies for low loss, high confinement silicon optical waveguides," J. Vacuum Sci. Technol. B 29, 06F309 (2011)

[2] Lukas Chrostowski, Michael Hochberg, chapter 12 in "Silicon Photonics Design: From Devices to Systems", Cambridge University Press, 2015

[3] http://siepic.ubc.ca/probestation, using Python code developed by Michael Caverley.

[4] Yun Wang, Xu Wang, Jonas Flueckiger, Han Yun, Wei Shi, Richard Bojko, Nicolas A. F. Jaeger, Lukas Chrostowski, "Focusing sub-wavelength grating couplers with low back reflections for rapid prototyping of silicon photonic circuits", Optics Express Vol. 22, Issue 17, pp. 20652-20662 (2014) doi: 10.1364/OE.22.020652

[5] www.plcconnections.com, PLC Connections, Columbus OH, USA.

[6] http://mapleleafphotonics.com, Maple Leaf Photonics, Seattle WA, USA.